


REGULAR ARTICLE



Ultraviolet Photodetector Based on Nanostructured Copper Iodide Films Deposited by Automatic SILAR Method

D. Fedonenko<sup>1</sup>, S.I. Petrushenko<sup>2,3,\*</sup> , K. Adach<sup>3</sup>, M. Fijalkowski<sup>3</sup>, V.M. Sukhov<sup>2</sup>, S.V. Dukarov<sup>2</sup>, A.L. Khrypunova<sup>1</sup>, N.P. Klochko<sup>1</sup>

<sup>1</sup> National Technical University "Kharkiv Polytechnic Institute", 61002 Kharkiv, Ukraine

<sup>2</sup> V.N. Karazin Kharkiv National University, 61022, Kharkiv, Ukraine

<sup>3</sup> Technical University of Liberec, 46117, Liberec, Czech Republic

(Received 18 January 2025; revised manuscript received 15 April 2025; published online 28 April 2025)

The paper presents the results of studies of the structure, composition and morphology of sulfur-doped copper iodide (CuI) nanostructured films deposited on glass substrates by the Successive Ionic Layer Absorption and Reaction (SILAR) method for use as functional materials for ultraviolet photodetectors (UV PD). By varying the temperature used in the deposition process, it is possible to obtain 1  $\mu\text{m}$  thick CuI layers with the morphology of nanoflakes (at 20 °C) or with (111)-textured triangular CuI nanograins (at 30 °C). By equipping these copper iodide layers with Cr/Cu thin film electrodes on both sides, we obtained UV PDs of photoconductive type. Their linear current-voltage characteristics confirmed the formation of ohmic contacts. The photoresponses of UV PDs over time were recorded and analyzed under different intensities from 0.15 mW/cm<sup>2</sup> to 1.17 mW/cm<sup>2</sup> of UV light with an average wavelength of 367 nm. According to the generally accepted criteria for evaluating the performance of a photodetector, the UV PD with the CuI nanoflake morphology has a higher performance and a shorter response time than that based on the nanostructured copper iodide film with triangular grains. It exhibits the photosensitivity of 170 %, the responsivity of 3 A/W, the specific detectivity of 1.2·10<sup>11</sup> Jones and the external quantum efficiency of 1000 %. These results are similar to those recently obtained by various research groups around the world, confirming the potential of using the UV photosensitive CuI material with nanoflake morphology obtained by the automatic SILAR method in thin-film UV sensing technology.

**Keywords:** Copper iodide, Ultraviolet photodetector, SILAR, Photosensitivity, Responsivity, Specific detectivity, External quantum efficiency.

DOI: [10.21272/jnep.17\(2\).02025](https://doi.org/10.21272/jnep.17(2).02025)

PACS numbers: 68.35. – p, 78.66. – w

1. INTRODUCTION

Ultraviolet (UV) light has both benefits and risks. Controlled exposure to UV radiation may be useful for sterilization, disinfection, and bone development in the body, but excessive exposure can lead to skin aging and, in severe cases, eye cataracts and skin cancer [1, 2]. Considering that UV radiation is beyond the range of the human eye, the development of various ultraviolet photodetectors (UV PDs) helps in detecting and using UV radiation for the benefit of humans. Moreover, UV PDs are needed for UV imaging, communication, and alarming, such as for use as electronic eyes [3] in door security systems used in garage door openers, and many other military and civilian applications [4, 5]. According to [1-5], wide-bandgap semiconductors with their highly efficient absorption of UV light and stable optoelectronic properties are ideal materials for UV PDs, in which UV photons can be converted into detectable signals in the form of electrical pulses, such as light current ( $I_{light}$ ). The prospects of using nanomaterials and nanostructures as active layers of UV photodetectors are justified by the ad-

vantages of low-dimensional wide-bandgap semiconductor nanostructures. First of all, this is their large specific surface area, which contributes to the formation of a network of channels for the transport of charge carriers (electrons and holes) under the influence of UV radiation, which ensures high photoconductivity recorded by UV PDs [5, 6]. Thus, ultraviolet photodetectors based on nanostructured wide-bandgap semiconductor films have attracted much attention in recent years due to their applications in military early warning, communication sensing, environmental monitoring and health care [1-6]. They can be divided into three types: photoconductive detectors, photovoltaic detectors and phototransistors based on different working principles. The simplest photoconductive type UV PDs are formed by using a thin-film wide-bandgap nanostructured semiconductor photoconductive material as a channel, and placing metal ohmic contacts as electrodes at both ends of this channel [2, 5].

Copper (I) iodide (CuI) is a *p*-type semiconductor material with a direct band gap of 2.95-3.1 eV [6, 7]. It has recently been used in various types of UV photodetectors [6-11], since the wide band gap of CuI helps to reduce

\* Correspondence e-mail: [Serhii.Petrushenko@tul.cz](mailto:Serhii.Petrushenko@tul.cz)



the dark current ( $I_{dark}$ ) that flows through photodetectors in the absence of UV light, thereby improving the signal-to-noise ratio [7]. CuI is a non-toxic, biocompatible, air-stable, promising for next-generation electronic devices p-type semiconductor with high electrical properties, visible transmittance and flexibility [7, 10]. Since CuI can be produced for UV PD using various methods such as solution processes [6-8, 11], vacuum deposition [7] and iodination processes [7, 9, 10], this makes it suitable for industry. The output characteristics of copper iodide-based ultraviolet photodetectors can be tuned by changing the morphology of the nanostructured films and their chemical composition [8]. For example, in [7] it is indicated that sulfur-doped CuI exhibits higher electrical conductivity with high optical transmittance.

Herein, we applied the solution automatic Successive Ionic Layer Adsorption and Reaction (SILAR) method to prepare sulfur-doped CuI nanostructured films on glass substrates. The influence of the temperature of solutions used in the SILAR method on the morphology of CuI nanostructures and their chemical composition was studied. For this purpose, CuI20/glass and CuI30/glass samples were obtained, in which copper iodide films were deposited using the SILAR method at solution temperatures of 20 °C and 30 °C, respectively. Then, by equipping the samples with two thin-film chromium electrodes, we constructed corresponding CuI20/glass and CuI30/glass UV PDs, and tested and compared their output characteristics.

## 2. EXPERIMENTAL PROCEDURES

In this work, the materials and automatic SILAR technology described recently in [12] were used to obtain CuI20/glass and CuI30/glass samples with nanostructured copper iodide films of  $\sim 1 \mu\text{m}$  thickness ( $d$ ) on glass substrates with an area of  $50 \text{ mm} \times 25 \text{ mm}$ . They were equipped along the two long sides of the samples with thin-film ohmic contacts obtained by successive vacuum evaporation through a mask of 50 nm thick Cr and 100 nm thick Cu films. The distance between two parallel thin-film Cr/Cu strip contacts ( $L$ ) was 2 cm. Due to the physical properties of chromium, the thin-film ohmic Cr/Cu contacts turned out to be stable under operating conditions. Additionally, these contacts were covered with self-adhesive aluminum tapes for connection to an external electrical circuit.

The morphology and chemical composition of CuI20/glass and CuI30/glass samples were studied by scanning electron microscopy (SEM) and energy-dispersive X-ray spectrometry (EDS) using a Zeiss ULTRA Plus SEM with a secondary electron (SE) mode equipped with an OXFORD X-Max 20 EDS detector providing elemental mapping. SEM images and EDS spectra were obtained using accelerating voltages in the range of 2-10 kV. The EDS maps of the samples were obtained as superpositions of the signal from the electron backscatter detector (colored white) and the intensities of the characteristic lines of individual elements, primarily Cu, I, and S, and colored in shades of the corresponding colors. The EDS maps were recorded with a resolution of  $500 \times 500$  pixels.

Tests of ultraviolet photodetectors of the photoconductive type CuI20/glass and CuI30/glass were carried out using a PHILIPS TL 6W/08 BLB G5 T5.226.3M ultraviolet lamp with an average wavelength of 367 nm as

a light source. The UV light intensity ( $P_{light}$ ) was adjusted from  $1.17 \text{ mW/cm}^2$  to  $0.15 \text{ mW/cm}^2$  by changing the distance between the UV lamp and the CuI20/glass or CuI30/glass sample in the range of 4.5-41 cm. At a bias voltage ( $V$ ) between two Cr/Cu strip contacts from 0 V to  $\pm 2$  V, the current-voltage characteristics ( $I$ - $V$ ) of the CuI20/glass and CuI30/glass samples were recorded using a GW Instek LCR-6002 meter indoors under normal sunlight illumination through a window glass that does not transmit ultraviolet light. The effective irradiation area ( $A$ ) of UV PD, which was limited by a screen with a slit width of 0.5 mm between the UV radiation source and the sample, was  $0.1 \text{ cm}^2$ . To obtain photoreponses of the CuI20/glass and CuI30/glass ultraviolet photodetectors at different  $P_{light}$  values, the change of the on/off ratio over time was recorded at  $V = 1 \text{ V}$  in air at room temperature. Resistance under UV illumination ( $R_{light}$ ) was calculated from the experimental data as  $V/I_{light}$ . According to [1, 13, 14], the response time ( $t_{response}$ ) was defined as the rise time of the response current under UV illumination from 10 % to 90 % of the maximum current  $I_{light}$ .

## 3. RESULTS

Figure 1(a) shows the SEM image of the CuI20/glass sample with nanostructured copper iodide film deposited on the glass substrate by the automatic SILAR method at a solution temperature of 20 °C. The nanoflake morphology of CuI with a large surface area is visible, and the thickness of each nanoflake is  $\sim 100 \text{ nm}$ . The copper iodide nanoflakes are oriented perpendicular to the substrate, so the thickness of the CuI layer is about  $1 \mu\text{m}$ . The EDS spectrum of the CuI20/glass sample in Figure 1(b) shows the elements copper, iodine, and sulfur from this film, and Si from the glass substrate. The presence of sulfur is typical for copper iodide films prepared by the SILAR method since the cationic solution contains an unstable thiosulfate component. The overall EDS map in Figure 1(c) and the corresponding elemental EDS maps in Figure 1(d, e, f) confirm the homogeneity of CuI due to the uniform distribution of Cu, I and S throughout the film. According to the uniform Si signals in the EDS map in Fig. 1(g), the CuI film in the CuI20/glass sample has no holes.

As can be seen in Fig. 2, the automatic SILAR method allows for a radical change in the morphology of the resulting CuI layers by changing the temperature of the solutions used. The CuI30/glass sample prepared by the automatic SILAR method by heating the solutions to 30 °C shows in Fig. 2(a) triangular crystalline grains randomly oriented in the (111) plane, which is typical for copper iodide  $\gamma$ -CuI, since {111} is the lowest energy surface in the cubic zinc blende structure [12].

The EDS spectrum of the CuI30/glass sample in Fig. 2(b) is similar to that of the CuI20/glass sample in Fig. 1(b), since it contains Cu, I, and S atoms from the nanostructured semiconductor layer, along with the main elements of the glass substrate. The overall EDS map in Fig. 2(c) of the CuI30/glass sample, the left side of which is covered with a thin-film Cr/Cu contact, as well as the elemental EDS maps in Fig. 2(d, e, f, g); confirms the uniform distribution of the nanostructured copper iodide film over the sample without micro-holes and cracks.

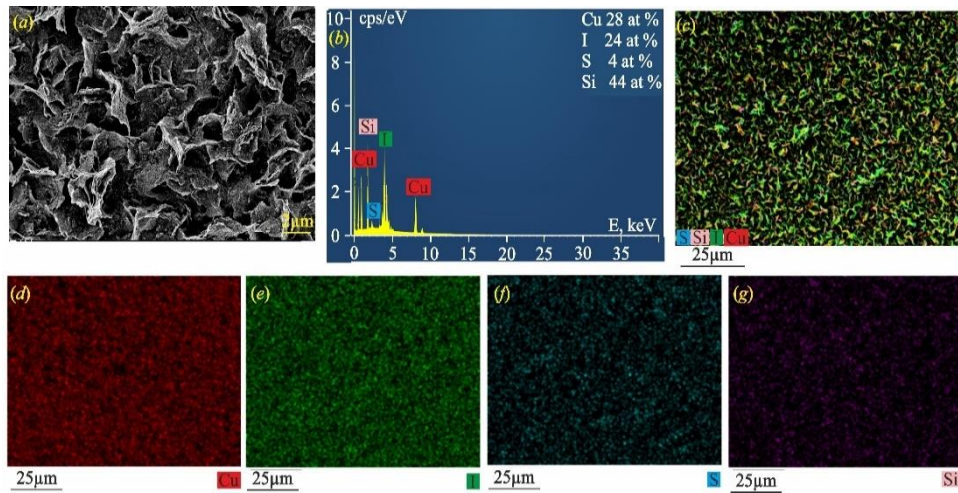


**Fig. 1** – Morphology and composition of the CuI20/glass sample obtained by the automatic SILAR method at a solution temperature of 20 °C: SEM image (a); EDS spectrum (b); general EDS map (c); EDS map for Cu (d); EDS map for I (e); EDS map for S (f); EDS map for Si (g)

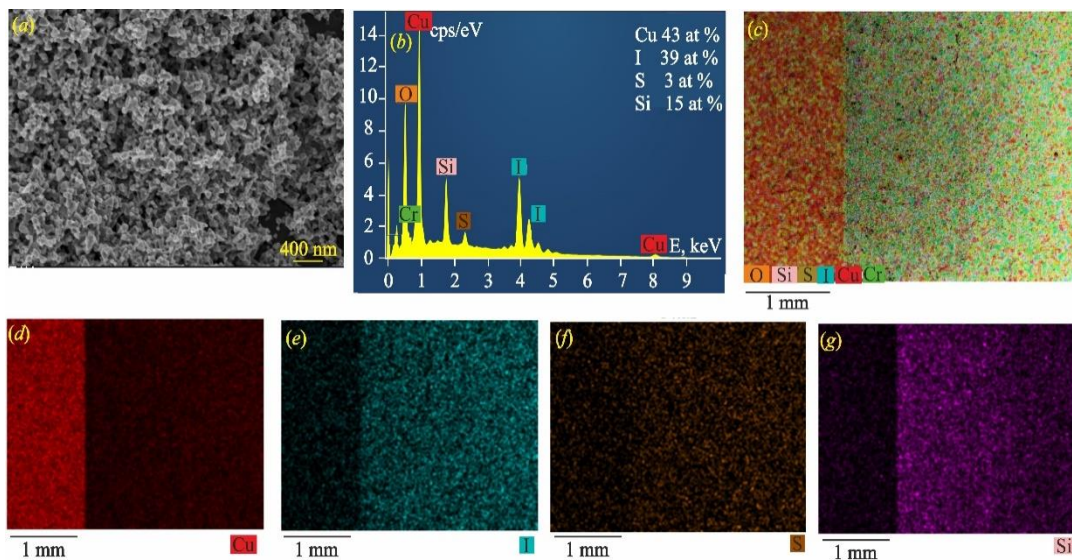


**Fig. 2** – Morphology and composition of the CuI30/glass sample obtained by the automatic SILAR method using solutions heated to 30 °C: SEM image (a); EDS spectrum (b); general EDS map of the CuI30/glass sample, which left part is covered by thin-film Cr/Cu contact (c); EDS map for Cu in this sample (d); EDS map for I in this sample (e); EDS map for S in this sample (f); EDS map for Si in this sample (g)

Linear current-voltage characteristics of the developed photoconductive type UV PDs based on CuI20/glass and CuI30/glass samples equipped with Cr/Cu thin-film electrodes confirm the creation of ohmic contacts. The conductivity of nanostructured CuI films was calculated using the distance between the electrodes ( $L$ ), its resistance in the absence of UV light ( $R_{dark}$ ), sample width ( $D$ ), and thickness of the CuI semiconductor layer:

$$\sigma = L / (R_{dark} \cdot D \cdot d), \quad (1)$$

Using the current-voltage characteristics, it was shown that the CuI film with nanoflake morphology in the CuI20/glass sample, obtained by the SILAR method at a solution temperature of 20 °C, has a significantly higher resistance compared to the CuI film with (111)-textured triangular grains, deposited by the SILAR

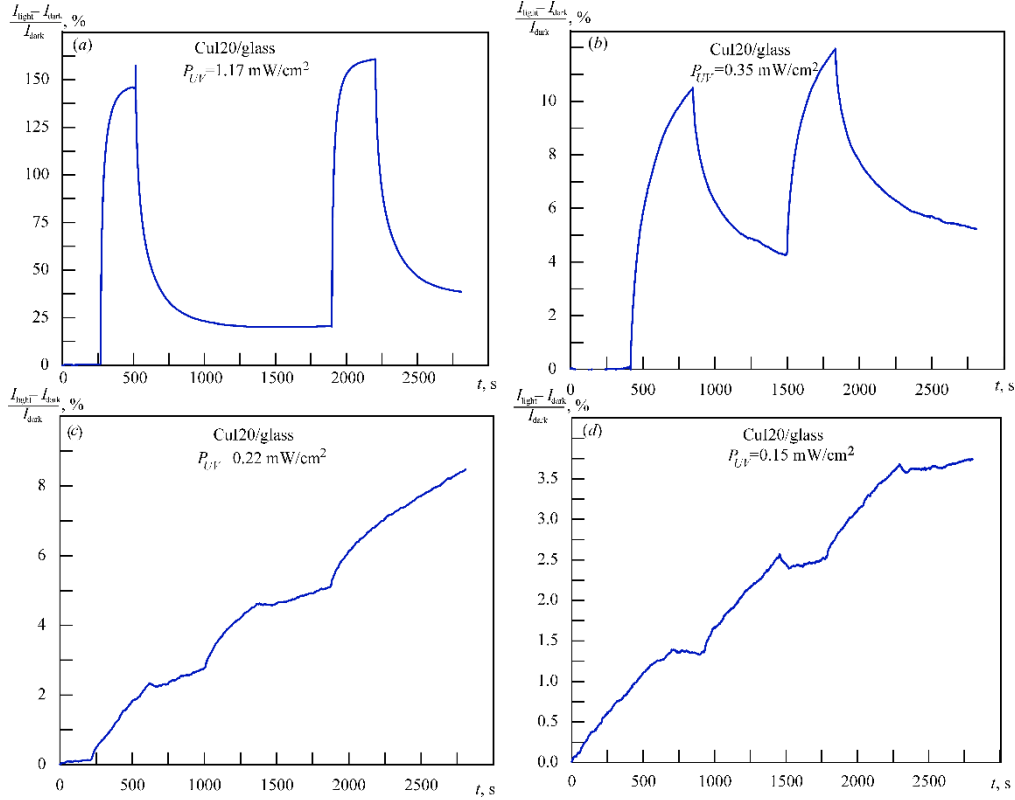
method at 30 °C in the CuI30/glass sample. The calculated  $\sigma$  value is  $\sim 0.05 \text{ S cm}^{-1}$  in the CuI20/glass sample, and  $\sigma \approx 22 \text{ S cm}^{-1}$  in the CuI30/glass sample. As noted in [15], the low resistance of copper iodide thin films with (111)-texture and triangular morphology can be due to the existence of conduction channels along the grain boundaries.

Fig. 3 and Fig. 4 show the photoresponses as relative change in resistance over time for the CuI20/glass and CuI30/glass ultraviolet photodetectors, respectively, at different intensities  $P_{light}$  of UV light with an average wavelength of 367 nm. The experiments were carried out indoors under normal sunlight illumination through a window glass that does not transmit ultraviolet light. It is evident in Fig. 3 and Fig. 4 that after turning on the UV light, due to the creation of nonequilibrium charge carriers as a result of ultraviolet irradiation of the wide-gap semiconductor CuI, its resistance decreases sharply. After turning off the

UV irradiation, the resistance immediately increases. This effect of UV light is stronger, the higher the value of  $P_{light}$ . In Fig. 3(a) and (b), it can be seen that in the CuI20/glass photodetector, well-defined signals are obtained at UV radiation intensities  $P_{light}$  of 1.17 mW/cm<sup>2</sup> and 0.35 mW/cm<sup>2</sup>. As shown in Fig. 3(c) and (d), at lower  $P_{light}$  of 0.22 mW/cm<sup>2</sup> and 0.15 mW/cm<sup>2</sup>, the visible light interferes with the detection of the UV signals. The signal of the CuI30/glass UV PD at  $P_{light}$  of 1.17 mW/cm<sup>2</sup> in Fig. 4(a) is not as strong as that of the CuI20/glass UV PD in Fig. 3(a). In addition,

a greater tendency for the detection accuracy of the UV light to decrease due to its interference with the visible light signals is recorded in Fig. 4(b) and (c) at lower  $P_{light}$  of 0.50 mW/cm<sup>2</sup> and 0.35 mW/cm<sup>2</sup>, respectively.

According to [2], high-performance ultraviolet detectors should have high sensitivity, quantum efficiency, and response speed, as well as signal-to-noise ratio. A comparative analysis of the performance parameters of CuI20/glass and CuI30/glass UV PDs was carried out using common criteria [1-3, 8, 13, 14].



**Fig. 3** – Photoresponses of CuI20/glass UV PD over time as a result of switching on/off UV light with  $\lambda \approx 367$  nm, recorded at a bias of 1 V at different UV illumination intensities  $P_{light}$ : 1.17 mW/cm<sup>2</sup> (a); 0.35 mW/cm<sup>2</sup> (b); 0.22 mW/cm<sup>2</sup> (c) and 0.15 mW/cm<sup>2</sup> (d)

According to [8, 14], the UV photosensitivity ( $S_{ph}$ ) of the photodetectors fabricated in this work, due to the wide band gap of CuI of about 3 eV, was calculated based on their photoresponse data as follows:

$$S_{ph} = \frac{I_{light} - I_{dark}}{I_{dark}} \cdot 100, \quad (2)$$

where  $I_{light}$  is the current under UV illumination and  $I_{dark}$  is the current without UV illumination in the room, both currents flow through the photodetector at a bias of 1 V.

Data on the photosensitivity of the CuI20/glass and CuI30/glass ultraviolet photodetectors at different UV illumination intensities are presented in Fig. 5 (a).

Fig. 5 (b) shows the data on the responsivity ( $R_{UV}$ ) as the ability to convert photons into electrons in photodetectors, calculated through the ratio of the photogenerated current to the power of the incident light. According to [1-3, 8, 13, 14] the  $R_{UV}$  value, related to the power density of incident light  $P_{light}$  and surface of the active layer  $A$ , was determined as follows:

$$R_{UV} = \frac{I_{light} - I_{dark}}{A \cdot P_{light}} \quad (3)$$

Since detectivity is a parameter describing the detection sensitivity of a photodetector against a noise background, when normalized by active area, it is defined as specific detectivity ( $D^*$ ) to compare the sensitivity between photodetectors with different device areas and bandwidths [2]. According to [1-3, 8, 13], the specific detectivity of the CuI20/glass and CuI30/glass UV PDs was calculated as:

$$D^* = R_{UV} \times (A / 2eI_{dark})^{1/2}, \quad (4)$$

where  $e$  is the electron charge. Data on  $D^*$  are presented in Fig. 5 (c).

The external quantum efficiency ( $EQE$ ) as the ratio of the number of collected photogenerated carriers to the number of incident photons, showing the ability of UV PD to convert a photon into a carrier, was calculated according to [1-3, 8, 13, 14] as follows:

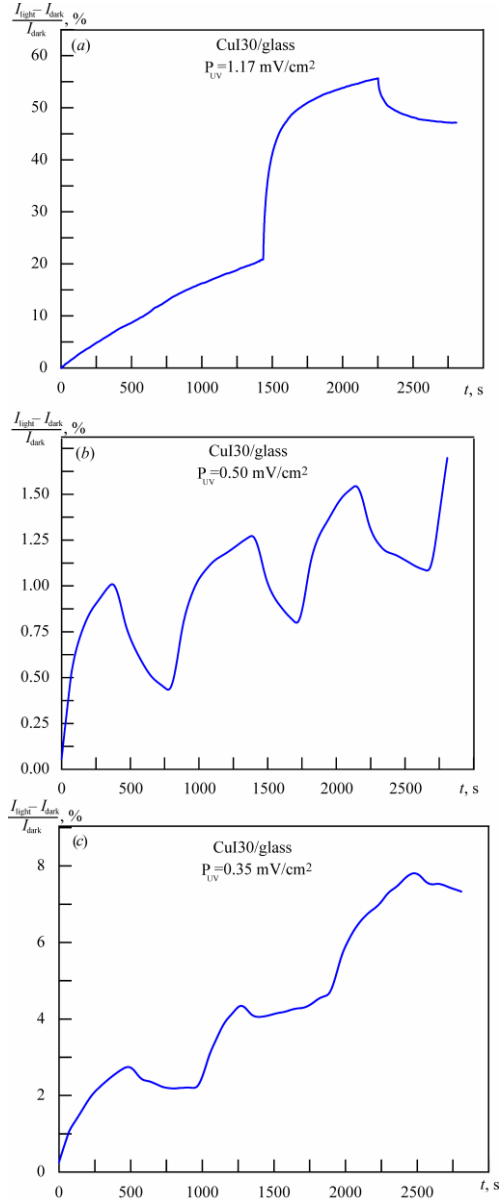


**Fig. 4** – Photoresponses of CuI30/glass UV PD over time as a result of switching on/off UV light with  $\lambda \approx 367 \text{ nm}$ , recorded at a bias of 1 V at different UV illumination intensities  $P_{light}$ : 1.17 mW/cm<sup>2</sup> (a); 0.50 mW/cm<sup>2</sup> (b); 0.35 mW/cm<sup>2</sup> (c)

$$EQE = \frac{R_{UV} \cdot h \cdot c}{e \cdot \lambda} \quad (5)$$

where  $h$  is Planck's constant,  $c$  is the speed of light, and  $\lambda$  is the wavelength of the incident UV radiation. The EQE data for both photodetectors are shown in Fig. 5(d).

According to the four criteria mentioned above, the CuI20/glass UV PD with CuI nanoflake morphology has a higher performance than the CuI30/glass UV PD based on the copper iodide nanostructured film with triangular grains. Moreover, the comparison of the photoresponse curves in Fig. 3 and Fig. 4 shows that the CuI20/glass

UV PD has a shorter response time defined as the rise time of the response current from 10 % to 90 % of the peak  $I_{light}$ . In the CuI20/glass UV photodetector, the  $t_{response}$  decreased from 300 s to 5 s with an increase in UV intensity from 0.15 mW/cm<sup>2</sup> to 1.17 mW/cm<sup>2</sup>. At the same time, the  $t_{response}$  in the CuI30/glass UV-PD was about 300 s for all  $P_{light}$  used. Thus, the morphology of CuI nanoflakes turned out to be favorable for use in photoconductive UV photodetectors compared to (111)-textured copper iodide films with triangular nanograins. Thus, according to [1, 2], the nanostructured CuI layer deposited by the automatic SILAR method at a temperature of 20 °C demonstrated better ability to convert optical signals into electrical signals by generating, separating, transmitting and recombining electron-hole pairs generated by UV light.

In general, the best characteristics of the CuI20/glass ultraviolet photodetector fabricated in this work were the photosensitivity  $S_{ph} \approx 170\%$ , responsivity  $R_{UV} \approx 3 \text{ A/W}$ , specific detectivity  $D^* \approx 1.2 \cdot 10^{11} \text{ Jones}$  (1 Jones =  $1 \text{ cm} \cdot \text{Hz}^{1/2} / \text{W}$ ), and external quantum efficiency  $EQE \approx 1000 \%$ . Comparison of these data with those obtained recently by various research groups around the world and presented in Table 1 confirms their validity.

#### 4. CONCLUSIONS

The results of scanning electron microscopy and energy-dispersive X-ray spectrometry studies of nanostructured copper iodide layers containing 3-4 at. % sulfur show that the automatic SILAR method allows for a fundamental change in their micromorphology by a simple small change in the temperature of the solutions used in the deposition process. Both CuI layers in the form of nanoflakes and layers consisting of triangular nanocrystalline grains randomly oriented in the (111) plane reversibly reduce their resistance under the action of UV radiation. The limitation of their photosensitivity to UV radiation with an illumination intensity of at least 0.5 mW/cm<sup>2</sup> is due to interference from visible light. According to four common performance criteria of photodetectors, such as photosensitivity, responsivity, specific detectivity and external quantum efficiency, the UV PD with 1  $\mu\text{m}$  thick CuI nanoflake layer on glass substrate equipped with two thin-film Cr/Cu ohmic stripe contacts has a performance comparable to the best state-of-the-art CuI-based UV PD. Its obvious drawback is the slow response, so the reduction of the response time by improving the PD design, such as replacing the ohmic contacts with Schottky barriers, should be carried out in our next study of the CuI-based UV PD.

#### ACKNOWLEDGEMENTS

The authors are grateful to the Ministry of Education and Science of Ukraine and the MSCA4Ukraine consortium funded under the EU Maria Skłodowska-Curie Program for ensuring the implementation of the work.

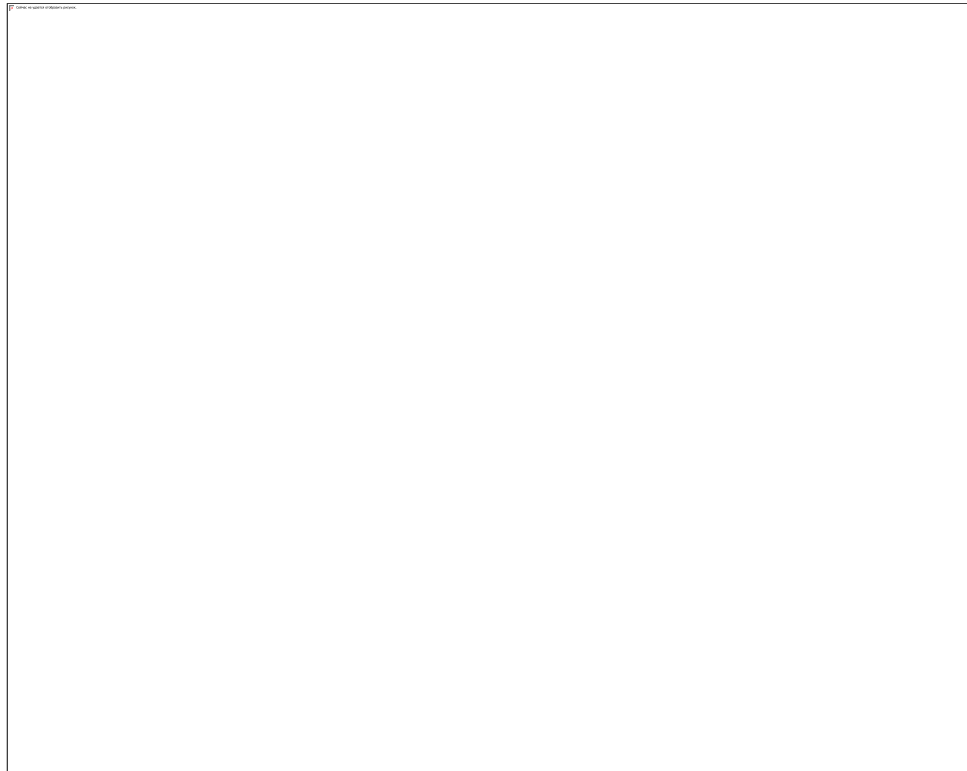


**Fig. 5** – Performance parameters of CuI20/glass and CuI30/glass UV PDs under different ultraviolet illumination intensities  $P_{light}$ : photosensitivity (a); responsivity (b); specific detectivity (c); external quantum efficiency (d)

**Table 1** – Photodetector properties of CuI-based UV PDs presented by different researchers

UV photodetector	Photosensitivity $S_{ph}$ , %	Responsivity, $R_{UV}$ , A/W	Specific detectivity $D^*$ , Jones	External quantum efficiency $EQE$ , %	Response time, $t_{response}$ , s	Reference
Zn-doped $p$ -CuI	–	0.72	$1.51 \times 10^8$	242	–	[7]
$p$ -CuI/ $n$ -GaN hetero-junction	–	0.08	$1.27 \times 10^{12}$	–	0.2	[7]
$n$ -ZnO/ $p$ -CuI	–	0.03	$2.21 \times 10^{12}$	–	0.2	[7]
Zn-doped $p$ -CuI	125	0.49	$3.01 \times 10^8$	164	–	[8]
$p$ -CuI/ $n$ -Si heterojunction	–	0.12	$5.7 \times 10^{12}$	–	0.1	[9]
$p$ -CuI / $n$ -Cu <sub>2</sub> O hetero-junction	7000	0.25	–	–	0.6	[11]
S-doped $p$ -CuI	170	2.97	$1.2 \times 10^{11}$	1007	5	[this work]

## REFERENCES

1. F. Cao, Y. Liu, M. Liu, Z. Han, X. Xu, Q. Fan, B. Sun, *Research* **7**, 0385 (2024).
2. W. Fang, Q. Li, J. Li, Y. Li, Q. Zhang, R. Chen, M. Wang, F. Yun, T. Wang, *Crystals* **13**, 915 (2023).
3. Y. Guo, Y. Li, Q. Zhang, H. Wang, *J. Mater. Chem. C* **5**, 1436 (2017).
4. H. Lin, A. Jiang, S. Xing, L. Li, W. Cheng, J. Li, W. Miao, X. Zhou, L. Tian, *Nanomaterials* **12**, 910 (2022).
5. A. Rogalski, Z. Bielecki, J. Mikołajczyk, J. Wojtas, *Sensors* **23**, 4452 (2023).
6. K.P. Beh, R. Abdalrheem, F.K. Yam, *2018 IEEE Student Conference on Research and Development (SCoReD) – Selangor, Malaysia (2018.11.26-2018.11.28)*.
7. G.H. Kim, J. Lee, K. Ahn, M.G. Kim, *Soft Sci.* **4**, 33 (2024).
8. C.-Y. Tsay, Y.-C. Chen, H.-M. Tsai, P. Sittimart, T. Yoshitake, *Materials* **15**, 8145 (2022).
9. Y. Huang, J. Tan, G. Gao, J. Xu, L. Zhao, W. Zhou, Q. Wang, S. Yuan, J. Sun, *J. Mater. Chem. C* **10**, 13040 (2022).
10. J.-H. Cha, D.-Y. Jung, *ACS Appl. Mater. Interfaces* **9**, 43807 (2017).
11. H.T.D.S. Madusanka, H.M.A.M. Herath, C.A.N. Fernando, *Sensor. Actuat. A: Phys.* **296**, 61 (2019).
12. S.I. Petrushenko, M. Fijalkowski, K. Adach, D. Fedonenko, Y.M. Shepotko, S.V. Dukarov, V.M. Sukhov, A.L. Khrypunova, N.P. Klochko, *Chemosensors* **13**, 29 (2025).
13. S. Sha, K. Tang, M. Liu, P. Wan, C. Zhu, D. Shi, C. Kan, M. Jiang, *Photon. Res.* **12**, 648 (2024).
14. M. Krishnaiah, A. Kumar, D. Mishra, A.K. Kushwaha, S.H. Jin, J.T. Park, *J. Alloy. Compd.* **887**, 161326 (2021).
15. T. Stralka, M. Bar, F. Schöppach, S. Selle, C. Yang, H. von Wenckstern, M. Grundmann, *phys. status solidi a* **220**, 2200883 (2023).

**Ультрафіолетовий фотодетектор на основі наноструктурованих плівок йодиду міді, нанесених автоматичним методом SILAR**

Д. Федоненко<sup>1</sup>, С.І. Петрушенко<sup>2,3</sup>, К. Адач<sup>3</sup>, М. Фіялковський<sup>3</sup>, В.М. Сухов<sup>2</sup>, С.В. Дукаров<sup>2</sup>,  
А.Л. Хрипунова<sup>1</sup>, Н.П. Клочко<sup>1</sup>

<sup>1</sup> *Національний технічний університет «Харківський політехнічний інститут», 61002 Харків, Україна*

<sup>2</sup> *Харківський національний університет імені В.Н. Каразіна, 61022 Харків, Україна*

<sup>3</sup> *Технічний університет Лібереця, 46117 Ліберець, Чеська Республіка*

У статті наведено результати досліджень структури, складу та морфології наноструктурованих плівок йодиду міді (CuI), легованих сіркою, нанесених на скляні підкладки методом послідовної адсорбції та реакції іонних шарів (SILAR) для використання у якості функціональних матеріалів для ультрафіолетових фотодетекторів (UV PD). Змінюючи температуру, що використовується в процесі осадження, можна отримати шари CuI товщиною 1 мкм із морфологією нанопластівців (при 20 °C) або з (111)-текстурованими трикутними нанозернами CuI (при 30 °C). Оснастивши ці шари йодиду міді тонкоплівковими електродами Cr/Cu з обох боків, ми отримали UV PD фотопровідного типу. Їх лінійна вольт-амперна характеристика підтвердила утворення омичних контактів. Фотовідгуки UV PD у часі реєстрували та аналізували при різних інтенсивностях УФ-світла із середньою довжиною хвилі 367 нм від 0,15 мВт/см<sup>2</sup> до 1,17 мВт/см<sup>2</sup>. Відповідно до загальноприйнятих критеріїв оцінки ефективності фотодетектора, UV PD з морфологією нанопластівців CuI має вищу продуктивність і менший час відгуку, ніж на основі наноструктурованої плівки йодиду міді з трикутними зернами. Він демонструє світлочутливість 170 %, монохроматичну ампер-ватну чутливість 3 А/Вт, специфічну детективність 1.2·10<sup>11</sup> Джонсів та зовнішню квантову ефективність 1000 %. Ці результати схожі на ті, що були нещодавно отримані різними дослідницькими групами в усьому світі, підтверджуючи потенціал використання УФ-світлочутливого матеріалу CuI з морфологією нанопластівців, отриманого автоматичним методом SILAR в технології тонкоплівкового ультрафіолетового зондування.

**Ключові слова:** Йодид міді, Ультрафіолетовий фотодетектор, SILAR, Фоточутливість, Монохроматична ампер-ватна чутливість, Специфічна детективність, Зовнішня квантова ефективність.